Supporting Information

Experimental Section

Determination of NH_3: The indophenol blue colorimetric method was used to determine NH_3 concentration in the electrolyte after reduction (the ultimate solution was diluted 20 times, 50 times, 100 times according to the actual situation). Specifically, it is necessary in this process to mix these solutions including 2 mL diluted electrolyte, 1 mL 0.05 M NaClO, 0.2 mL sodium nitroprusside (1 wt%) and 2 mL of 1 M NaOH coloring solution containing 5% salicylic acid and 5% sodium citrate. Relevant UV-vis absorption spectra of mixed solutions were obtained after being placed in darkness for 2h, using the absorbance at 655 nm to identify NH_3 concentration. The concentration-absorbance curve was calibrated using the standard NH_4Cl solution with NH_3 concentrations of 0.25, 0.5, 1.0, 2.5, 5.0 ppm in 0.1 M NaOH solution. Decent linear relation of absorbance value with NH_3 concentration is shown in the fitting curve ($y = 0.21x - 0.079$, $R^2 = 0.999$).

Determination of N_2H_4: The Watt and Chrisp method is used to estimate N_2H_4 production. In short, it is necessary to mix 5 mL solution required detection and 5 mL color reagent from the mixed solution containing 5.99 g $C_9H_{11}NO$, 30 mL HCl and 300 mL ethanol. The absorbance of the solution was detected at 455 nm after stirring at room temperature for 10 min. Excellent linear relation of absorbance value with N_2H_4 concentration is shown in the fitting curve ($y = 0.563x + 0.014$, $R^2 = 0.999$).

Calculations of NH_3 yield and FE: The NH_3 yield was calculated according to the following equation: $R_{NH3} = (m_{NH3})/(t \times S)$, where m_{NH3} signifies the total mass of NH_3, t represents the reaction duration, and S is the immersed area of the sample. Faradaic efficiency (FE) was calculated according to the equation: $FE = 6F \times n_{NH3}/Q$, where F means the Faraday constant and Q is the total quantity of applied electricity.

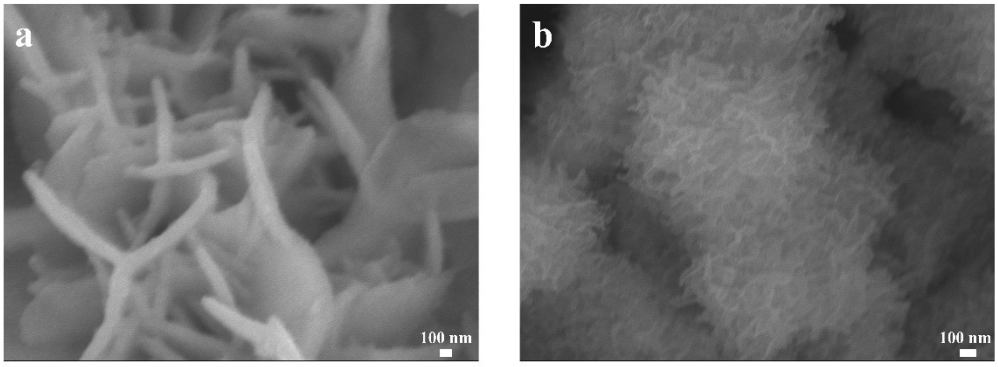

Fig. S1. SEM images of (a) Co_3O_4/NiFe LDH-20 and (b) Co_3O_4/NiFe LDH-60.

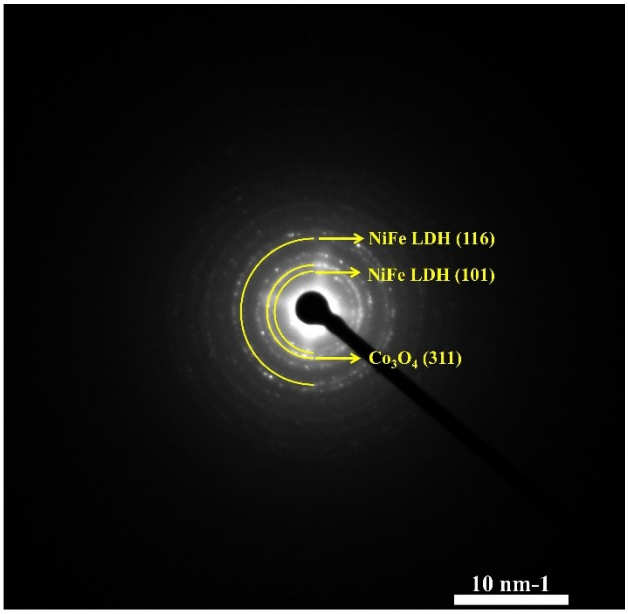

Fig. S2. SAED pattern of Co_3O_4/NiFe LDH-40.

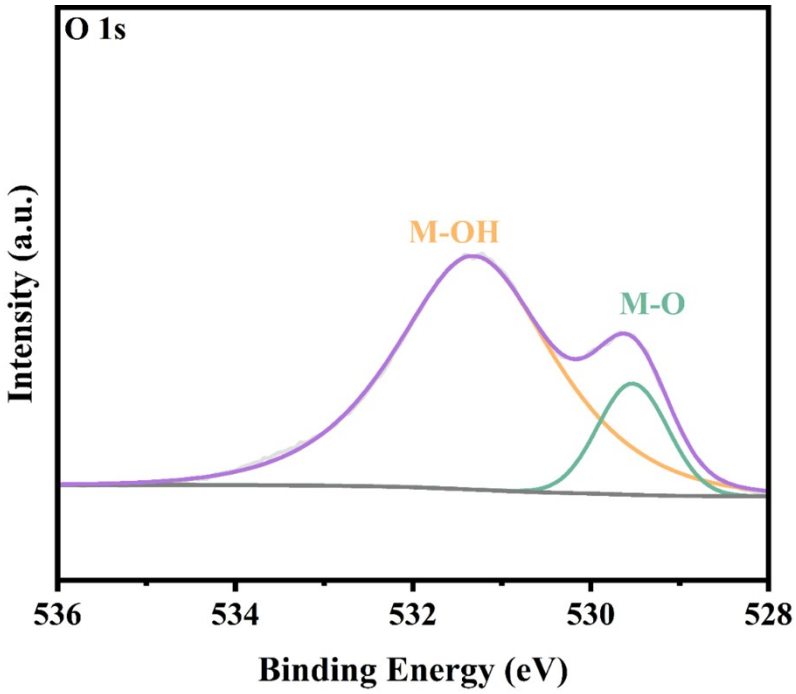

Fig. S3. O 1s XPS spectrum of Co_3O_4/NiFe LDH-40.

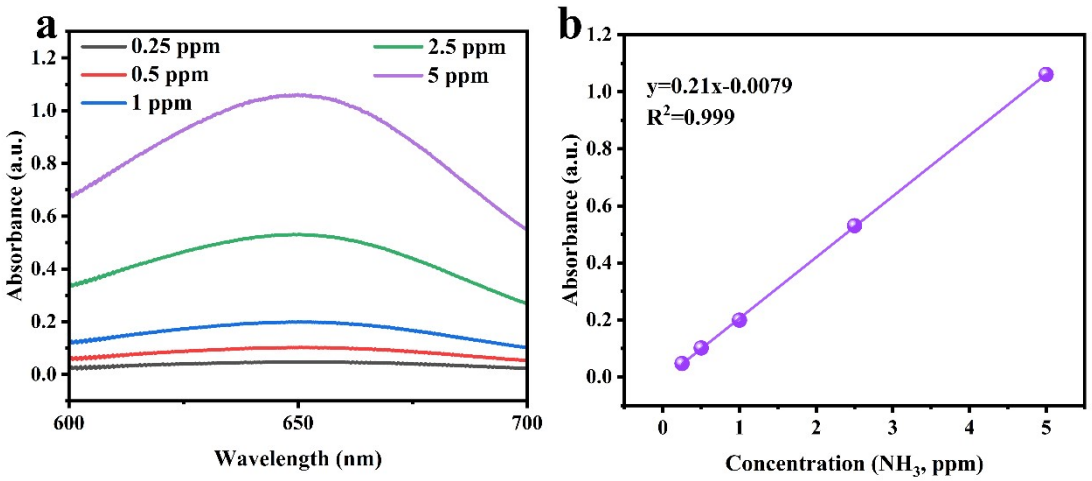

Fig. S4. (a) UV–vis absorption spectra and (b) corresponding calibration curve for calculation of NH_4^+ concentration.

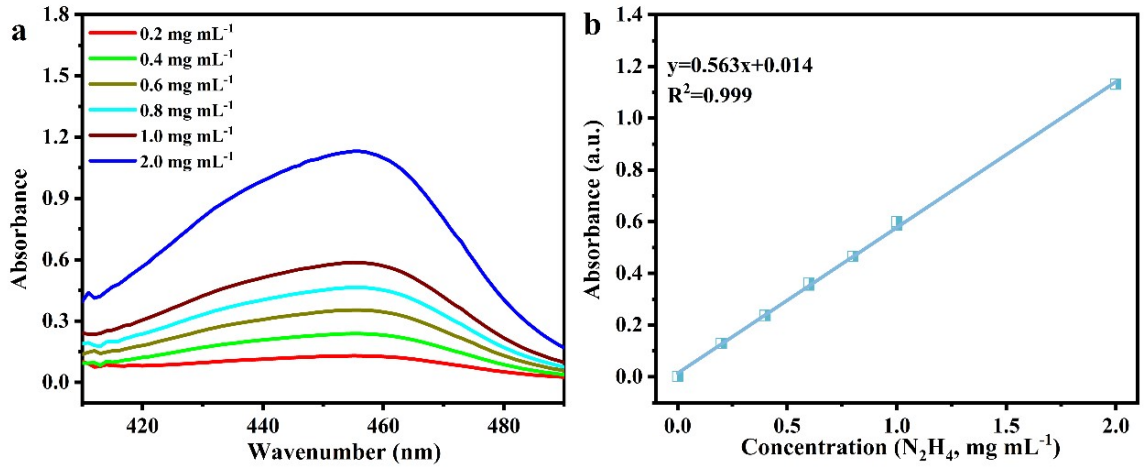

Fig. S5. (a) UV–vis absorption spectra and (b) corresponding calibration curve for calculation of N_2H_4 concentration.

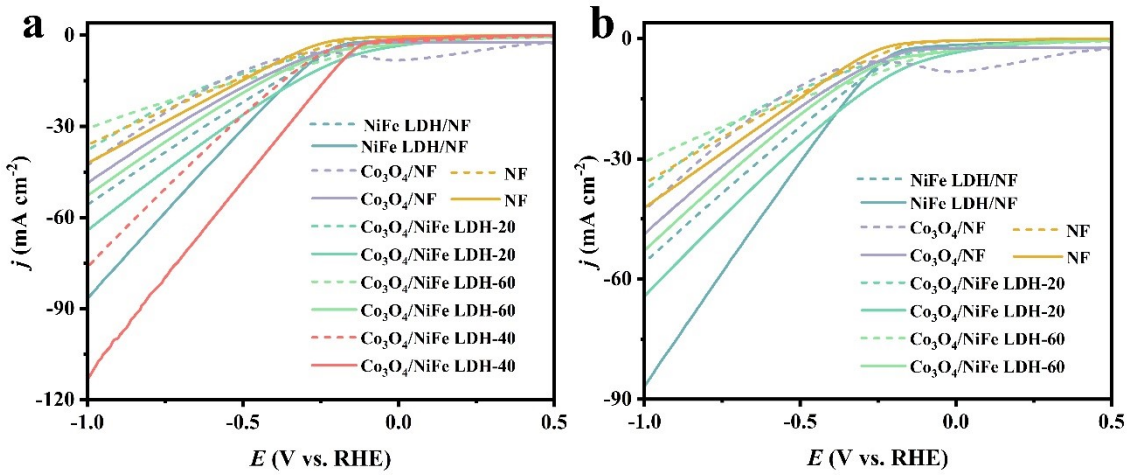

Fig. S6. (a) LSV curves of various catalysts, (b) amplified LSV curves of the comparison samples in NO_2^--containing and NO_2^--free 0.1 M NaOH (The dotted line represents the condition in NO_2^--containing 0.1 M NaOH, solid line represents the condition in NO_2^--free 0.1 M NaOH).

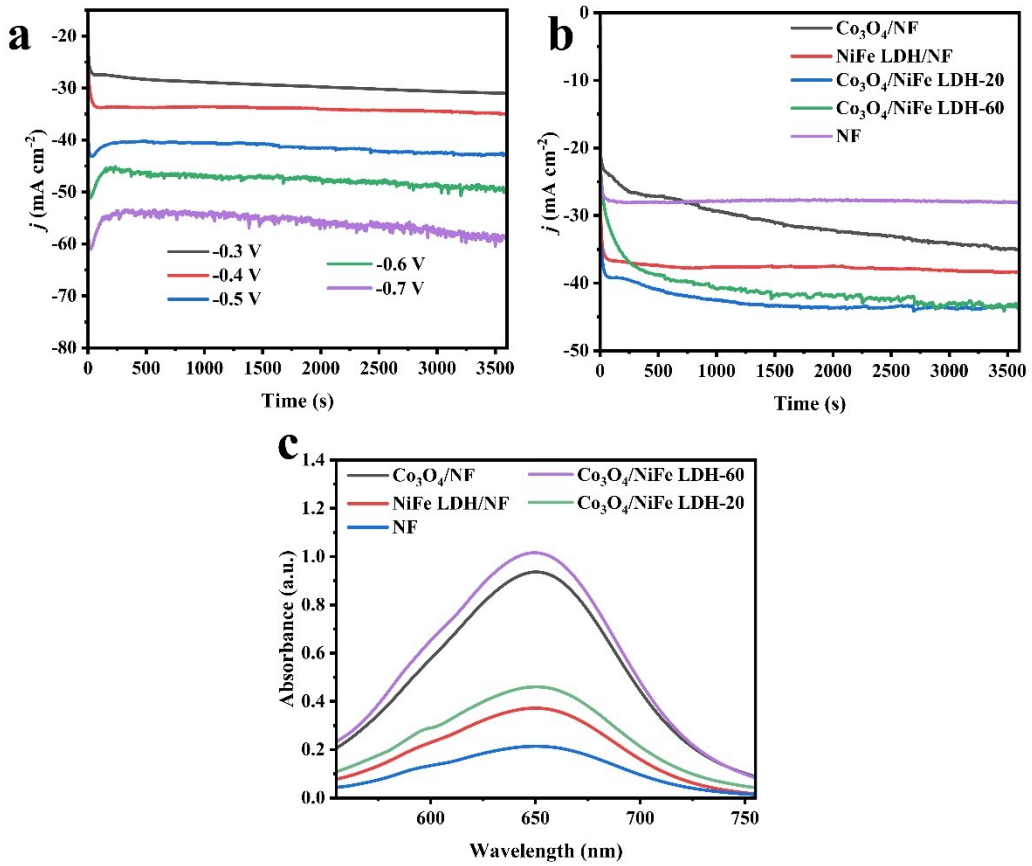

Fig. S7. Chronoamperometry curves of (a) Co_3O_4/NiFe LDH-40 at different applied potentials and (b) Co_3O_4/NF, NiFe LDH/NF, Co_3O_4/NiFe LDH-20, Co_3O_4/NiFe LDH-60 and NF at -0.5 V. (c) UV–vis absorption spectra of NH_3 for Co_3O_4/NF, NiFe LDH/NF, Co_3O_4/NiFe LDH-20, Co_3O_4/NiFe LDH-60 and NF at -0.5 V.

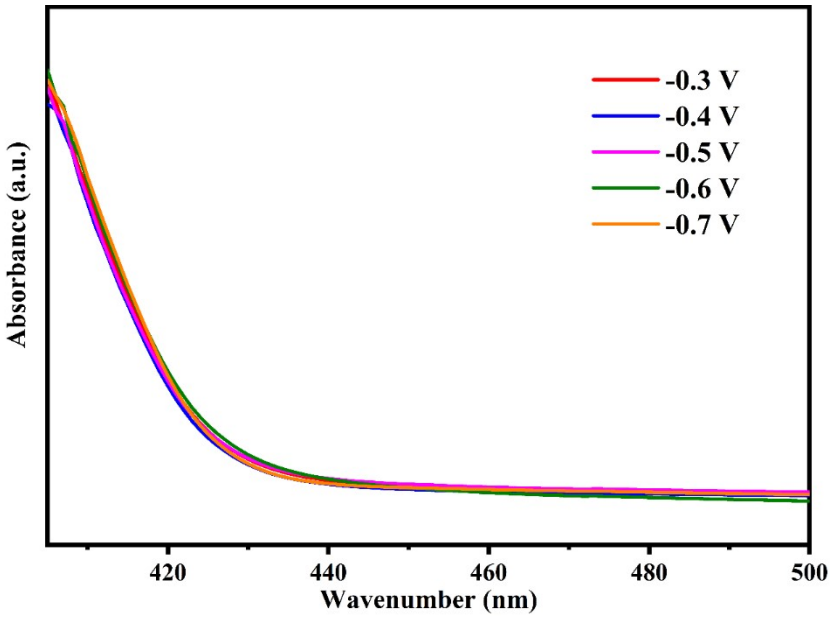

Fig. S8. UV–vis absorption spectra of N_2H_4 for Co_3O_4/NiFe LDH-40 at different potentials.

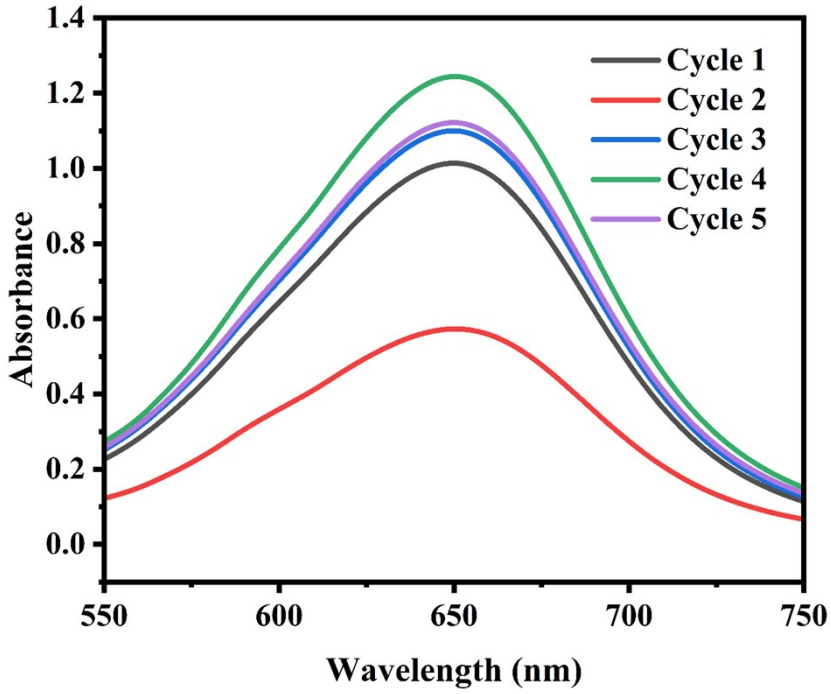

Fig. S9. UV–vis absorption spectra of NH_3 of Co_3O_4/NiFe LDH-40 during electrolysis. (The electrolyte from the cycle 1 is diluted 20 times, the electrolyte from the cycle 2 to the cycle 4 is diluted 50 times, and the electrolyte from the cycle 5 is diluted 100 times)

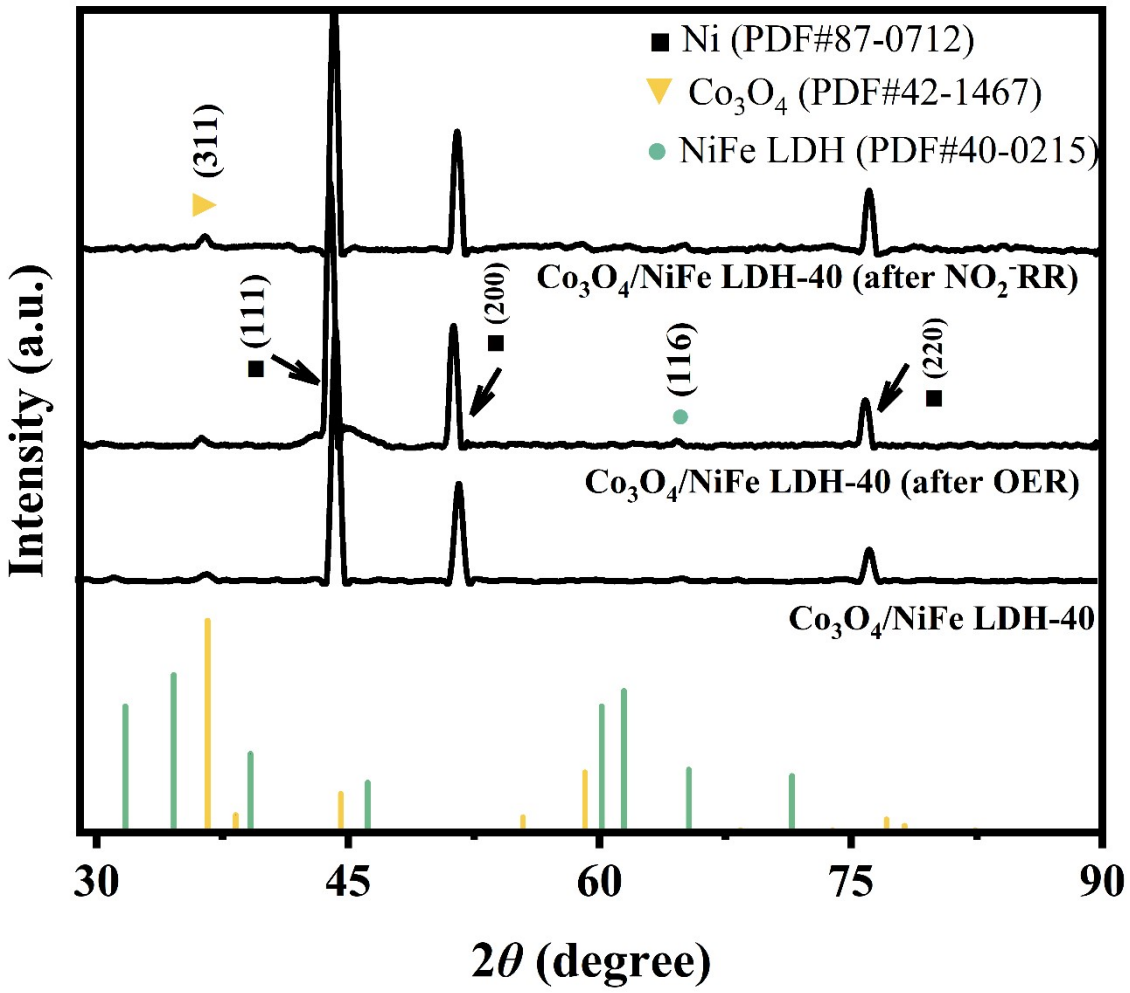

Fig. S10. XRD pattern of Co_3O_4/NiFe LDH-40, Co_3O_4/NiFe LDH-40 after OER and Co_3O_4/NiFe LDH-40 after NO_2^-RR

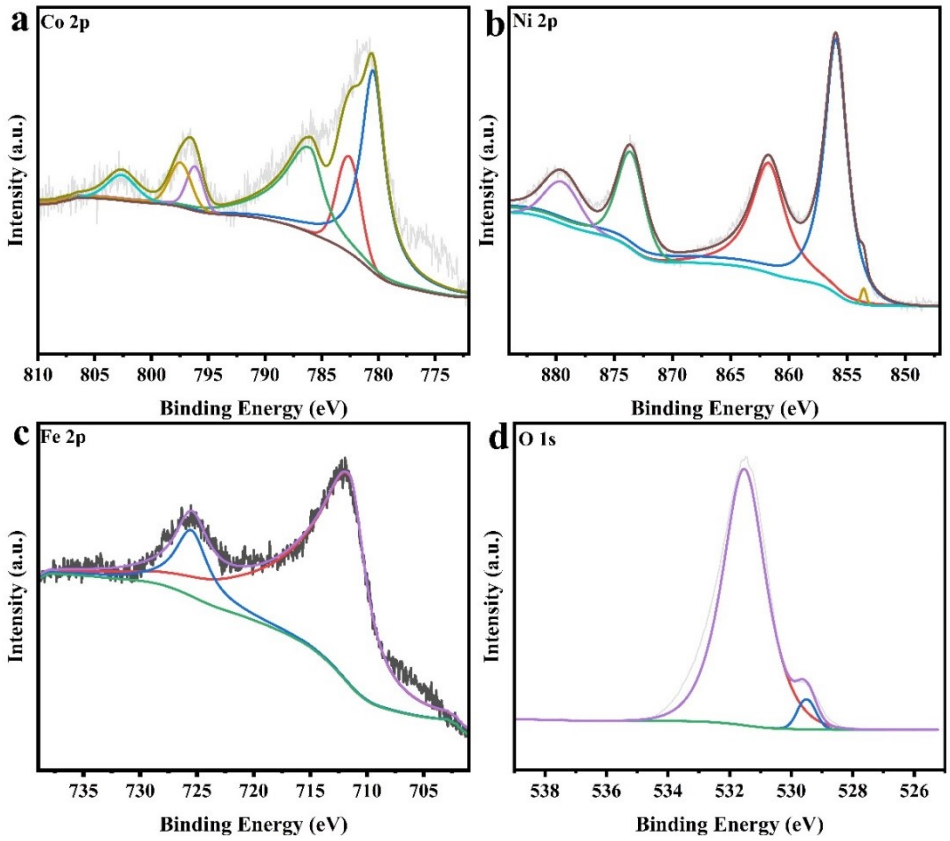

Fig. S11. (a) Co 2p, (b) Ni 2p, (c) Fe 2p and (d) O 1s XPS spectrum of Co_3O_4/NiFe LDH-40 after NO_2^-RR durability test.

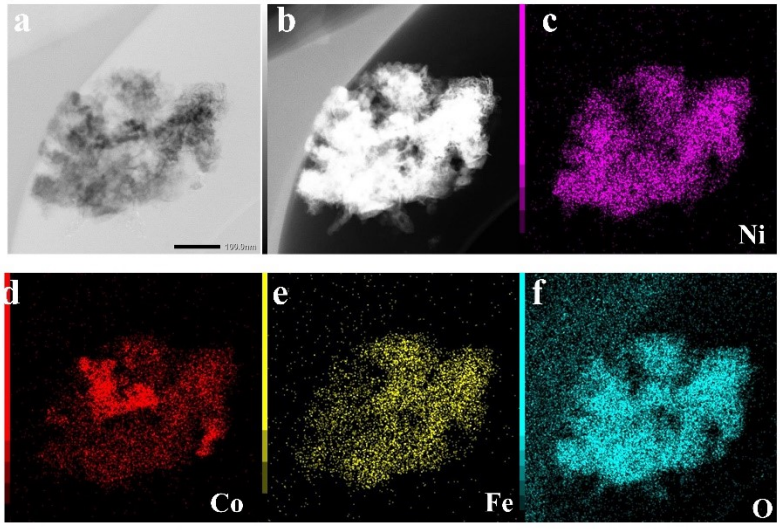

Fig. S12. (a)TEM, (b-g) corresponding elemental mapping images of Co_3O_4/NiFe LDH-40 after NO_2^-RR test.

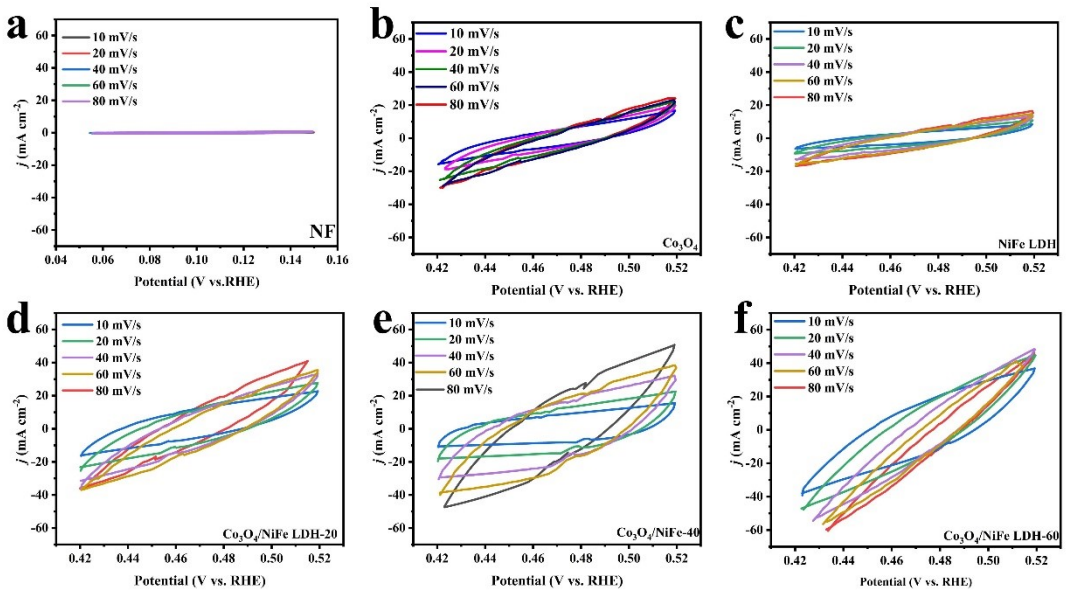

Fig. S13. Cyclic voltammetry curves of different catalysts tested at various scan rates ranging from 10 to 80 mV s^{-1}.

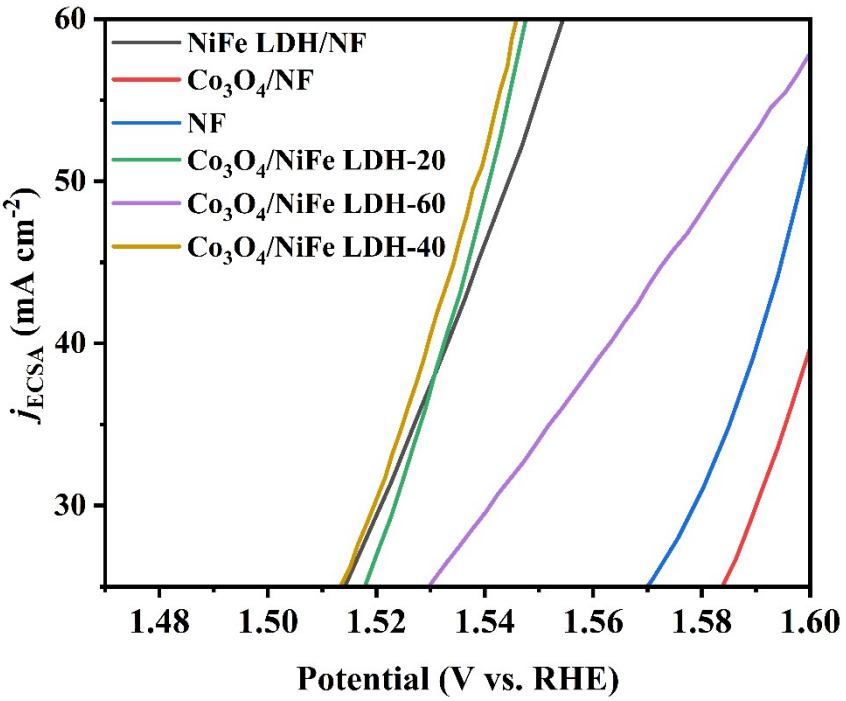

Fig. S14. Polarization curves of different catalysts based on ECSA.

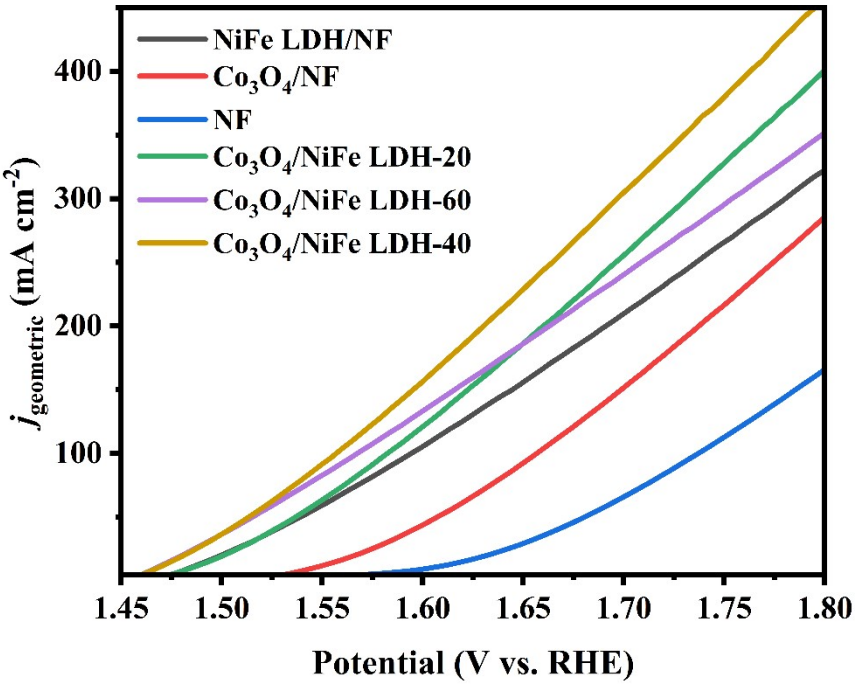

Fig. S15. Polarization curves of different catalysts based on geometric area without *iR* corrections.

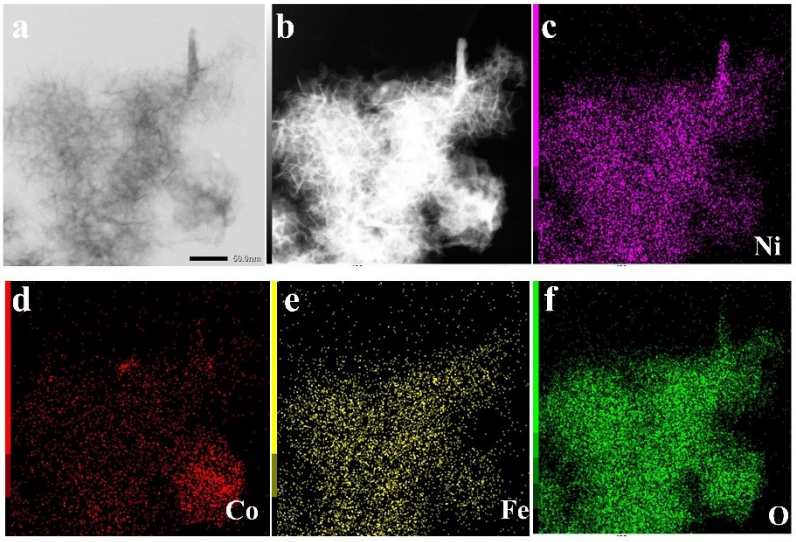

Fig. S16. (a)TEM, (b-g) corresponding elemental mapping images of Co_3O_4/NiFe LDH-40 after OER test.

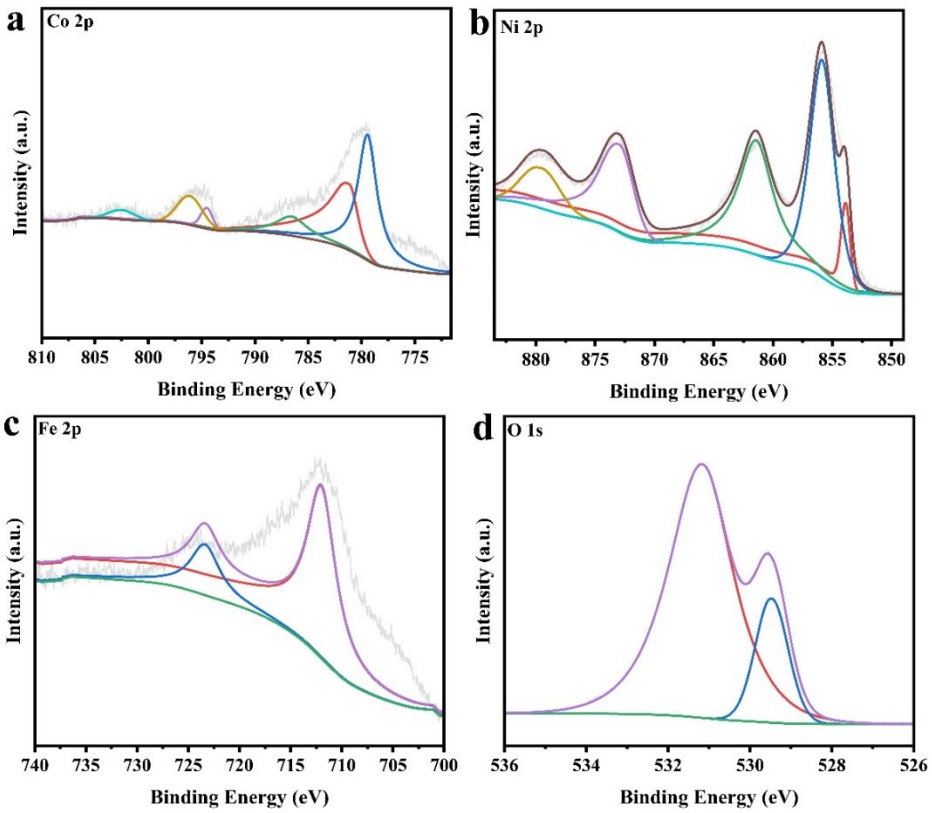

Fig. S17. (a) Co 2p, (b) Ni 2p, (c) Fe 2p and (d) O 1s XPS spectrum of Co_3O_4/NiFe LDH-40 after OER test.

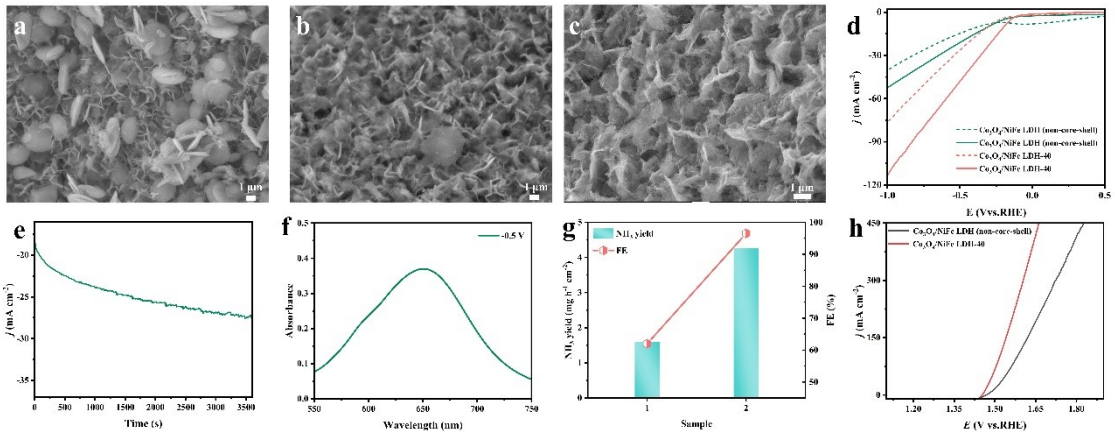

Fig. S18. SEM images of (a) non-core-shell Co_3O_4/NiFe LDH, (b) non-core-shell Co_3O_4/NiFe LDH after NO_2^-RR and (c)non-core-shell Co_3O_4/NiFe LDH after OER. (d) LSV curves of the samples in NO_2^--containing and NO_2^--free 0.1 M NaOH (The dotted line represents the condition in NO_2^--containing 0.1 M NaOH, solid line represents the condition in NO_2^--free 0.1 M NaOH). (e) i-t curve and (f) UV–vis absorption spectrum of

non-core-shell Co_3O_4/NiFe LDH at -0.5V. (g) comparison of NO_2^-RR performance in 1 (non-core-shell Co_3O_4/NiFe LDH), 2 (Co_3O_4/NiFe LDH-40). (h) OER performance comparison in samples.

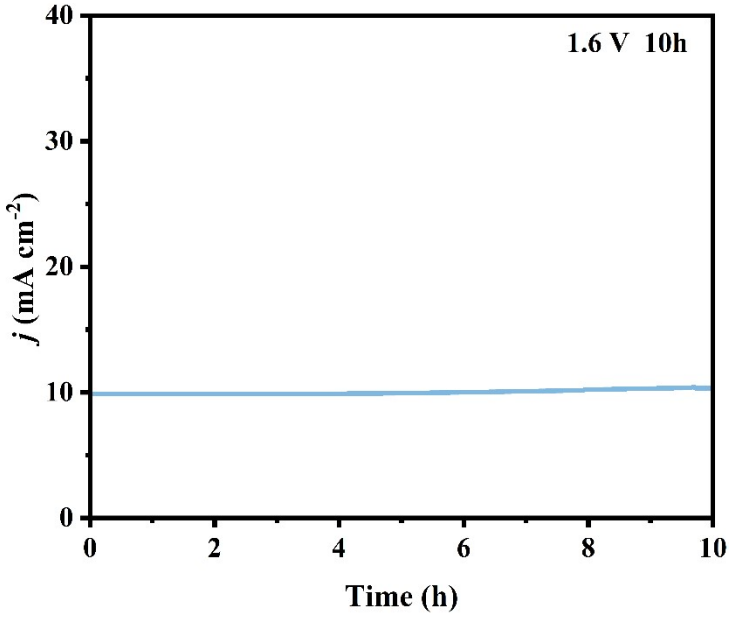

Fig. S19. Long-term stability of Co_3O_4/NiFe LDH-40 at OER||NO_2^-RR system.

Table S1. Comparison of NH_3 yield and FE of Co_3O_4/NiFe LDH-40 with other reported advanced electrocatalysts for nitrate reduction to produce ammonia.

Catalyst	Electrolyte	NH_3 yield ($mg\ h^{-1}\ cm^{-2}$)	FE (%)	Potential (V vs. RHE)	Ref.
Co_3O_4/NiFe LDH-40	**0.1 M OH^-+0.1 M NO_2^-**	**4.27**	**96.53**	**−0.5**	**This work**
Pd-doped TiO_2	1 M LiCl + 0.25 M $LiNO_3^-$	1.12	92.1	−0.7	[1]
Ni-NSA-VNi	0.2 M Na2SO4 + 200 ppm NO_2^-	4.011	96.1	−0.54	[2]
Cu3P NA/CF	0.1 M PBS + 0.1 M NO_2^-	1.626	91.2	−0.5	[3]
CoB nanoarray	0.2 M Na2SO4 + 400 ppm NO_2^-	3.962	95.2	−0.7	[4]
Ag@NiO/CC	0.1 M OH^-+0.1 M NO_2^-	2.295	75.8	−0.4	[5]
MoFe protein	0.25 M HEPES + 0.05 M NO_2^-	3.978	~100	−0.57 V	[6]
Ni2P nanosheet	0.1 M PBS + 200 ppm NO_2^-	2.69	87	−0.3	[7]

Table S2. Comparison of the OER performance for Co_3O_4/NiFe LDH-40 with other reported OER electrocatalysts in 1 M alkaline electrolyte.

Catalyst	η_{100} (mV)	η_{10}(mV)	Tafel Slope ($mV\ dec^{-1}$)	Reference
Co_3O_4/NiFe LDH-40	**280**	**234**	**48.4**	**This work**
Co_3O_4/NF	370	309	95.04	This work
NiFe LDH/NF	310	249	213.08	This work
NiFeRu–LDHs	/	225	31	[8]

Li^+- NiFe LDH	224	154	47.9	[9]
Ni_3S_2-NiFe LDHs/NF	/	205	35.6	[10]
B,N-GQDs/NiFe LDH	251	/	34	[11]
MIM-CoFe LDH	291.3	216.8	58.5	[12]
CoxFeyO-N	350	304	52.7	[13]
CoO/CeO_2	/	291	84	[14]

REFERENCES:

1. Guo Y, Zhang R, Zhang S, Zhao Y, Yang Q, Huang Z, Dong B, Zhi C. Pd doping-weakened intermediate adsorption to promote electrocatalytic nitrate reduction on TiO2 nanoarrays for ammonia production and energy supply with zinc–nitrate batteries. *Energy Environ Sci*. 2021;14:3938-3944. DOI: 10.1039/d1ee00806d.
2. Wang C, Zhou W, Sun Z, Wang Y, Zhang B, Yu Y. Integrated selective nitrite reduction to ammonia with tetrahydroisoquinoline semi-dehydrogenation over a vacancy-rich Ni bifunctional electrode. *J Mater Chem A Mater*. 2021;9:239-243. DOI: 10.1039/D0TA09590G.
3. Liang J, Deng B, Liu Q, Wen G, Liu Q, Li T, Luo Y, Alshehri AA, Alzahrani KA, Ma D, et al. High-efficiency electrochemical nitrite reduction to ammonium using a Cu3P nanowire array under ambient conditions. *Green Chem*. 2021;23:5487-5493. DOI: 10.1039/D1GC01614H.
4. Hu L, Zhao D, Liu C, Liang Y, Zheng D, Sun S, Li Q, Liu Q, Luo Y, Liao Y, et al. Amorphous CoB nanoarray as a high-efficiency electrocatalyst for nitrite reduction to ammonia. *Inorg Chem Front*. 2022;9:6075-6079. DOI: 10.1039/D2QI01363K.
5. Liu Q, Wen G, Zhao D, Xie L, Sun S, Zhang L, Luo Y, Ali Alshehri A, Hamdy MS, Kong Q, et al. Nitrite reduction over Ag nanoarray electrocatalyst for ammonia synthesis. *J Colloid Interface Sci*. 2022;623:513-519. DOI: https://doi.org/10.1016/j.jcis.2022.04.173.
6. Milton RD, Abdellaoui S, Khadka N, Dean DR, Leech D, Seefeldt LC, Minteer SD. Nitrogenase bioelectrocatalysis: heterogeneous ammonia and hydrogen production by MoFe protein. *Energy Environ Sci*. 2016;9:2550-2554. DOI: 10.1039/C6EE01432A.
7. Wen G, Liang J, Zhang L, Li T, Liu Q, An X, Shi X, Liu Y, Gao S, Asiri AM, et al. Ni2P nanosheet array for high-efficiency electrohydrogenation of nitrite to ammonia at ambient conditions. *J Colloid Interface Sci*. 2022;606:1055-1063. DOI: https://doi.org/10.1016/j.jcis.2021.08.050.
8. Zhang B, Zhu C, Wu Z, Stavitski E, Lui YH, Kim T, Liu H, Huang L, Luan X, Zhou L, et al. Integrating Rh Species with NiFe-Layered Double Hydroxide for Overall Water Splitting. *Nano Lett*. 2020;20:136-144. DOI: 10.1021/acs.nanolett.9b03460.
9. Lin X, Cao S, Chen X, Chen H, Wang Z, Liu H, Xu H, Liu S, Wei S, Lu X. Two Birds with One Stone: Contemporaneously Boosting OER Activity and Kinetics for Layered Double Hydroxide Inspired by Photosystem II. *Adv Funct Mater*. 2022;32:2202072. DOI: https://doi.org/10.1002/adfm.202202072.
10. Wu S, Liu S, Tan X, Zhang W, Cadien K, Li Z. Ni3S2-embedded NiFe LDH porous nanosheets with abundant heterointerfaces for high-current water electrolysis. *Chem Eng J*. 2022;442:136105. DOI: https://doi.org/10.1016/j.cej.2022.136105.
11. Rinawati M, Wang Y, Huang W, Wu Y, Cheng Y, Kurniawan D, Haw S, Chiang W, Su W, Yeh M. Unraveling the efficiency of heteroatom-doped graphene quantum dots incorporated MOF-derived bimetallic layered double hydroxide towards oxygen evolution reaction. *Carbon N Y*. 2022;200:437-447. DOI: https://doi.org/10.1016/j.carbon.2022.08.067.
12. Hu L, Tian L, Ding X, Wang X, Wang X, Qin Y, Gu W, Shi L, Zhu C. p–d hybridization in CoFe LDH nanoflowers for efficient oxygen evolution electrocatalysis. *Inorg Chem Front*.

2022;9:5296-5304. DOI: 10.1039/D2QI01688E.
13. Du Q, Su P, Cao Z, Yang J, Price CAH, Liu J. Construction of N and Fe co-doped CoO/CoxN interface for excellent OER performance. *Sustain Mater Technol*. 2021;29:e293. DOI: https://doi.org/10.1016/j.susmat.2021.e00293.
14. Liu H, Duan H, Yu J, Qiu C, Yu R, Gao J, Li S, Du X, Si Z, Yang S. Strong Electron Coupling Effect at the CoO/CeO2 Interface Enables Efficient Oxygen Evolution Reaction. *ACS Mater Lett*. 2022;4:2572-2578. DOI: 10.1021/acsmaterialslett.2c00802.